Technical Report # MBS2021-2-UIC
Department of Mechanical and Industrial Engineering
University of Illinois at Chicago

March 2021
(Version 2, updated July, 2021)

FRENET OSCILLATIONS AND FRENET-EULER ANGLES: CURVATURE SINGULARITY AND MOTION-TRAJECTORY ANALYSIS

Ahmed A. Shabana (shabana@uic.edu)
Department of Mechanical and Industrial Engineering
University of Illinois at Chicago
842 West Taylor Street
Chicago, Illinois 60607, USA

Abstract

A mechanics-based description of *motion-trajectory* (MT) curves is used in this investigation to introduce *Frenet oscillations*. These oscillations define the time-varying orientation of the *motion plane* that contains the absolute velocity and acceleration vectors in terms of three *Frenet-Euler angles*; the *curvature*, *vertical-development*, and *bank angles*, referred to as the *Frenet angles* for brevity. The Frenet bank angle and the associated *Frenet super-elevation* of the motion plane, which measure the deviation of the centrifugal inertia force from the horizontal plane, can be used to shed light on the definition of the *balance speed* used in practice. The concept of the *pre-super-elevated osculating (PSEO) plane* is introduced and *Rodrigues' formula* is employed to develop an orthogonal rotation matrix that provides a geometric interpretation of the PSEO plane. A new *inverse-dynamics problem* that utilizes experimentally or simulation *recorded motion trajectories* (RMT) is used to define the *Frenet inertia forces* and demonstrate their equivalence to the Cartesian form of the inertia forces. New expressions for the curvature vector in terms of the velocity and acceleration, limit on the magnitude of the tangential acceleration for a given forward velocity, condition required for the centrifugal force to remain horizontal, and condition of *curvature singular points* that corresponds to zero absolute acceleration are derived. The Frenet bank angle can be used to prove the existence of the normal vectors at the curvature singular points. It is shown that the inertia force can assume different forms, depending on the curve parameter used, and if the arc length parameter is not used as the curve parameter, the inverse-problem equation can include a quadratic-velocity inertia force vector. The results of a simple analytical curve demonstrate the concept of the *Frenet oscillations* and importance of distinguishing between the highway-ramp and railroad *track bank angles* and super-elevations, which are time-invariant, and the *Frenet bank angle* and super-elevation, which are motion-dependent.

Keywords: Frenet oscillations; Frenet-Euler angles; motion trajectories; curvature singularity; centrifugal inertia forces; recorded motion trajectories.

1. Introduction

Linear and nonlinear vibrations are motion characteristics of a wide class of physics and engineering systems [1 – 7]. For this reason, understanding and controlling these vibrations have been the subject of many investigations [8 – 12]. Nonetheless, in the performance evaluation of physics and engineering systems, the actual forces that produce the oscillations during the system functional operations are not a priori known. Therefore, experimentally-and computer-simulation-recorded *motion trajectories* (MT) will become increasingly important for understanding the motion of complex systems and for providing interpretation of the actual forces that produce this motion. Sophisticated equipment and sensors in modern vehicles and machines and advanced computer-simulation technology allow obtaining accurate *recorded-motion trajectories* (RMT) using sensor measurements or credible and detailed virtual-prototyping computer models.

The analysis of the RMT curves, therefore, can contribute to better understanding and proper interpretation of the forces that produce the actual motion. Such an analysis lies at the intersection of two important fields; *nonlinear dynamics* and *computational mechanics*. The qualitative nonlinear-dynamics techniques can be used effectively in the analysis of large amount of data obtained using computational algorithms. Furthermore, techniques of differential and computational geometry are needed to properly interpret the RMT-curve geometries [13 – 18]. This is particularly important because forces such as the inertia forces can have different interpretation depending on the generalized coordinates used [19 – 24]. *D'Alembert-Lagrange principle* leads to different definitions and interpretations of the inertia forces depending on the coordinates used to formulate the dynamic equations of motion.

To better understand RMT data, physics-based interpretation of the geometry is required. To this end, *Frenet-Euler angles*, called Frenet angles for brevity, are used to describe arbitrary curve

geometries, and are explicitly defined in terms of the curve derivatives which can be determined from recorded coordinates, velocities, and accelerations. As discussed in this paper, any curvilinear motion, regardless of the geometry of the highway road or railroad track, leads to centrifugal forces that do not appear in the classical Newton-Euler equations in their Cartesian form. Balancing these forces can be crucial in ensuring stability and safe operation of vehicle systems. Understanding direction of the inertia forces and extracting useful information from RMT data require using new concepts and definitions such as the *Frenet super-elevation* and *Frenet bank angle*, which vary with time and define orientation of the *osculating motion plane* that contains the velocity and acceleration vectors.

To demonstrate the need for the analysis of the RMT-curve geometry, the method used to define the vehicle operating speeds during curve negotiations is considered. To ensure a safe operation of highway and railroad vehicles during curve negotiations, a *super-elevation* is used to define a *balance speed* at which the vehicle must operate. The goal is to create a lateral gravity force that balances the lateral component of the centrifugal inertia force [24 – 26]. This lateral force balance is based on the assumption that the vehicle strictly traces a circular curve that lies in a plane parallel to the horizontal plane. Figure 1 shows such a curve, denoted as curve C, which has normal vector $\mathbf{n}_C$ that defines the direction of the centrifugal force under the above-mentioned condition. Such a condition of circular curve, however, cannot be met in realistic motion scenarios because of a lateral vehicle motion. If the vehicle traces another curve D, with normal $\mathbf{n}_D$ different from $\mathbf{n}_C$, the centrifugal force does not lie in a plane parallel to the horizontal plane and the assumption used in defining the balance speed is violated. Such curve examples demonstrate the value of the RMT curve analysis in identifying root causes of accidents and derailments.

This paper is focused on addressing the important issue of the RMT curve analysis, and developing mechanics-based interpretation of the curve geometry. The specific contributions and organization of the paper are summarized as follows:

1. The paper generalizes the concept of the *Frenet angles* for the description of arbitrary curve geometry by building on previous recent investigations [25 – 26]. In Sections 2 and 3, the Frenet angles, which are the *curvature*, *vertical-development*, and *bank angles*, are expressed in terms of the derivatives of the curve defined in its parametric form to give them a geometric interpretation. It is shown that the curvature vector that defines the direction of the centrifugal force can be written as a linear combination of two orthogonal unit vectors that define the normal and curvature vectors before performing the Frenet bank rotation. To this end, the concept of the *pre-super-elevated osculating (PSEO) plane* is introduced. *Rodrigues' formula* is used to obtain the rotation matrix required to perform the orthogonal transformation that explains the PSEO-plane orientation.
2. The condition required for the centrifugal force to remain in a plane parallel to the horizontal plane and the condition of curvature singularities are discussed in Section 4. It is shown that a curve can be Frenet vertically-elevated but not Frenet super-elevated. Because the curve curvature is defined to be the magnitude of the curvature vector, the existence of the normal vector at the *curvature singular point* is an issue that can be addressed using the Frenet angles. A proof of the existence of the normal vector at the curvature singular points is provided.
3. A new *inverse problem* based on experimentally or simulation *recorded motion trajectories* (RMT) is defined. The *Frenet inertia forces* are defined and their equivalence to the Cartesian form is demonstrated in Section 5. The curve geometric description is used to define the tangential and normal inertia-force components which lie in the osculating plane. In the special

case of constant forward velocity, new expressions for the curvature vector in terms of the velocity and acceleration are presented and the limit on the magnitude of the tangential acceleration for a given forward velocity is derived. Discussion on the assumption of horizontal centrifugal force used to define the *balance speed* is also provided in Section 5.

4. The forms of the equations of motion used in the inverse problem based on the RMT curves are developed. It is shown that the inertia force can assume different forms, depending on the curve parameter used. As demonstrated in Section 6, if the arc length parameter is not used as the curve parameter, the inverse-problem equation can include a quadratic-velocity inertia force vector, shedding light on the importance of proper interpretation of the inertia forces when different coordinates are used.
5. A new procedure is introduced in Section 7 to explain the steps required to extract the geometry and force variables from the RMT curves. It is shown that the RMT curves can be used to obtain different forms of the equations of motion and the forces that appear in these equations. The centrifugal force in its totality can be determined, and the lateral and vertical components often used to study railroad vehicle derailments are readily available from the information extracted from the RMT curves.
6. Regardless of the geometry and orientation of the highway roads and railroad tracks, lateral vehicle displacements can result in tracing motion curves with large curvature and sharp radius of curvature that can be smaller than the minimum track radius of curvature mandated by federal regulations. To better explain the problem, an analytical curve is used to demonstrate the concept of the *Frenet oscillations* in Section 8. The time-varying oscillations of the *Frenet osculating plane*, due to the change in the Frenet bank angle, define the direction of the centrifugal forces; shedding light on the limitations of the method used in practice to define

the balance speed based on the assumption of a horizontal centrifugal force, an assumption often violated. The results presented in Section 8 also explain the importance of distinguishing between the *track bank angle* and super-elevation, and the *Frenet bank angle* and super-elevation of the osculating (motion) plane, respectively. While tangent tracks are designed with zero track super-elevation, motion-dependent Frenet super-elevation cannot be avoided on tangent tracks because of the hunting oscillations [24].

Section 9 provides more discussion on the Frenet bank angle and the curvature singularity, and explains relationship between the analysis presented in this investigation and previous studies. Summary and conclusions drawn from this study are provided in Section 10. While an analytical curve is used in Section 7, future investigations will be concerned with developing more detailed railroad vehicle models to explain the importance of distinguishing between the oscillatory Frenet angles and the time-invariant Euler angles used in the description of the railroad track geometry.

2. General curve geometry

Without any loss of generality, the relationship between the Cartesian form and the *Frenet form* of the inertia forces can be explained using the spatial curve written in its parametric form as $\mathbf{r} = \begin{bmatrix} x & y(x) & z(x) \end{bmatrix}^T$. The curve is defined using the parameter x, which is assumed different from the curve arc length s. Basic geometry equations that are repeatedly used in this paper are summarized in Section 2.1.

2.1 Tangent and curvature vectors

The *tangent vector* is defined as $\mathbf{r}_x = \partial \mathbf{r}/\partial x = \begin{bmatrix} 1 & y' & z' \end{bmatrix}^T$, where $y' = \partial y/\partial x$ and $z' = \partial z/\partial x$. The norm of this vector is $|\mathbf{r}_x| = \sqrt{1 + (y')^2 + (z')^2}$. Therefore, the unit tangent to the curve is defined as

$$\mathbf{r}_s = \partial\mathbf{r}/\partial s = \begin{bmatrix} 1 & y' & z' \end{bmatrix}^T \Big/ \left|\mathbf{r}_x\right| \tag{1}$$

Furthermore, one has the differential relationship $ds = \left|\mathbf{r}_x\right| dx$, or alternatively $\partial s/\partial x = \left|\mathbf{r}_x\right| = \sqrt{1+\left(y'\right)^2+\left(z'\right)^2}$. It follows that $\partial\left(1/\left|\mathbf{r}_x\right|\right)/\partial x = -\left(y'y''+z'z''\right)/\left|\mathbf{r}_x\right|^3$.

The *curvature vector* is $\mathbf{r}_{ss} = \partial^2\mathbf{r}/\partial s^2 = \left(\partial\left(\begin{bmatrix} 1 & y' & z' \end{bmatrix}^T/\left|\mathbf{r}_x\right|\right)/\partial x\right)\left(\partial x/\partial s\right)$, which can be written using the equation $\partial x/\partial s = 1/\left|\mathbf{r}_x\right|$ as $\mathbf{r}_{ss} = \left(1/\left|\mathbf{r}_x\right|\right)\left(\partial\left(\begin{bmatrix} 1 & y' & z' \end{bmatrix}^T/\left|\mathbf{r}_x\right|\right)/\partial x\right)$. This equation yields

$$\begin{aligned} \mathbf{r}_{ss} &= \frac{1}{\left|\mathbf{r}_x\right|^4}\left(-\left(y'y''+z'z''\right)\begin{bmatrix} 1 \\ y' \\ z' \end{bmatrix} + \left(1+\left(y'\right)^2+\left(z'\right)^2\right)\begin{bmatrix} 0 \\ y'' \\ z'' \end{bmatrix}\right) \\ &= \frac{1}{\left|\mathbf{r}_x\right|^4}\begin{bmatrix} -\left(y'y''+z'z''\right) \\ y''+z'\left(y''z'-y'z''\right) \\ z''+y'\left(z''y'-z'y''\right) \end{bmatrix} = \frac{1}{\left|\mathbf{r}_x\right|^2}\begin{bmatrix} -\alpha_c \\ y''-\alpha_c y' \\ z''-\alpha_c z' \end{bmatrix} \end{aligned} \tag{2}$$

where $\alpha_c = \left(y'y''+z'z''\right)/\left|\mathbf{r}_x\right|^2$. The *curvature* κ, magnitude of the curvature vector, is defined as

$$\begin{aligned} \kappa = \kappa\left(x\right) &= \sqrt{\left(\alpha_c\right)^2+\left(y''-\alpha_c y'\right)^2+\left(z''-\alpha_c z'\right)^2}\Big/\left|\mathbf{r}_x\right|^2 \\ &= \sqrt{\left(\left(y''\right)^2+\left(z''\right)^2\right)-\left(\alpha_c\right)^2\left|\mathbf{r}_x\right|^2}\Big/\left|\mathbf{r}_x\right|^2 \end{aligned} \tag{3}$$

This equation for the curvature can be written as

$$\begin{aligned} \kappa = \kappa\left(x\right) &= \sqrt{\left(y''\right)^2+\left(z''\right)^2-\left(\alpha_c\right)^2\left|\mathbf{r}_x\right|^2}\Big/\left|\mathbf{r}_x\right|^2 \\ &= \sqrt{\left(\left(y''\right)^2+\left(z''\right)^2\right)\left|\mathbf{r}_x\right|^2-\left(y'y''+z'z''\right)^2}\Big/\left|\mathbf{r}_x\right|^3 \\ &= \sqrt{\left(y''\right)^2\left(1+\left(z'\right)^2\right)+\left(z''\right)^2\left(1+\left(y'\right)^2\right)-2y'z'y''z''}\Big/\left|\mathbf{r}_x\right|^3 \end{aligned} \tag{4}$$

Using this equation, the radius of curvature of the curve at an arbitrary point x can be written as $R = R\left(x\right) = 1/\kappa\left(x\right)$. The unit tangent vector $\mathbf{r}_s$ and the unit normal vector $\mathbf{n} = \mathbf{r}_{ss}/\kappa$ define the

osculating (*motion*) *plane* which is the plane of the velocity and acceleration vectors that enter into the definition of the inertia forces.

To define the torsion, the bi-normal vector must be determined and differentiated with respect to the arc length. The bi-normal vector can be determined as the cross product of the unit tangent and normal vectors. The definition of the torsion in terms of Euler angles was provided in [25]. The curve torsion, however, does not play a role in the development presented in this paper.

2.2 Geometric interpretation

One can also show that the curvature vector $\mathbf{r}_{ss}$ can be written as a linear combination of two orthogonal vectors $\mathbf{n}_1$ and $\mathbf{n}_2$ as

$$\mathbf{r}_{ss} = \kappa_h \mathbf{n}_1 + \kappa_v \mathbf{n}_2 = \frac{\kappa_h}{\sqrt{1+(y')^2}} \begin{bmatrix} -y' \\ 1 \\ 0 \end{bmatrix} + \frac{\kappa_v}{|\mathbf{r}_x|\sqrt{1+(y')^2}} \begin{bmatrix} -z' \\ -y'z' \\ 1+(y')^2 \end{bmatrix} \tag{5}$$

where

$$\left.\begin{aligned} \kappa_h &= y'' \Big/ |\mathbf{r}_x|^2 \sqrt{1+(y')^2}\,, \\ \kappa_v &= \left(z''\left(1+(y')^2\right) - z'y'y''\right) \Big/ \left(|\mathbf{r}_x|^3 \sqrt{1+(y')^2}\right), \\ \mathbf{n}_1 &= \left(1 \Big/ \sqrt{1+(y')^2}\right)\begin{bmatrix} -y' & 1 & 0 \end{bmatrix}^T, \\ \mathbf{n}_2 &= \left(1 \Big/ |\mathbf{r}_x|\sqrt{1+(y')^2}\right)\begin{bmatrix} -z' & -y'z' & 1+(y')^2 \end{bmatrix}^T \end{aligned}\right\} \tag{6}$$

It is worth mentioning that the vectors $\mathbf{n}_1$ and $\mathbf{n}_2$ are functions of the first derivatives only and do not depend on the second derivatives of the curve. Using the definitions of the preceding equation, and the orthogonality of the unit vectors $\mathbf{n}_1$ and $\mathbf{n}_2$, the curve curvature can be written as

$$\kappa = \sqrt{(\kappa_h)^2 + (\kappa_v)^2} = \frac{\sqrt{(y'')^2 |\mathbf{r}_x|^2 + \left(z''\left(1+(y')^2\right) - z'y'y''\right)^2}}{|\mathbf{r}_x|^3 \sqrt{1+(y')^2}} \tag{7}$$

It can be shown that this expression of the curvature is the same as the expression previously obtained in this section. The two curvature expressions demonstrate that the curvature can assume different forms in terms of the first and second derivatives of the curve coordinates. The analysis presented in this section can also be used to write the normal vector as

$$\mathbf{n} = \left(\kappa_h / \kappa\right)\mathbf{n}_1 + \left(\kappa_v / \kappa\right)\mathbf{n}_2 \tag{8}$$

This equation will be used in the following section to introduce the *Frenet angles*.

2.3 Curvature singular points

In the classical differential geometry, a point on a curve is called a *singular point* if $\left|\mathbf{r}_x\right| = 0$ or equivalently $\left|\mathbf{r}_s\right| = 0$. Based on the analysis presented in this section, a *curvature singular point* is defined as a point at which $y'' = z'' = 0$. At curvature singular points, $\alpha_c = \left(y'y'' + z'z''\right)\Big/\left|\mathbf{r}_x\right|^2 = 0$, and $\kappa_h = \kappa_v = \kappa = 0$. It will be shown that at the curvature singular points of RMT curves, the tangential acceleration $\ddot{s}$ is equal to zero, that is $\ddot{s} = 0$. It is worth mentioning that the condition $y'' = z'' = 0$ is derived with the assumption that x is the curve parameter. If another curve parameter is selected, this condition can assume a different form. It is also worth mentioning that zero curvature does not imply that the derivative of the curvature is zero, that is, $\kappa = 0$ does not always imply that $\kappa' = 0$. At the curvature singular points, the unit vector normal to curve cannot be determined by dividing the curvature vector $\mathbf{r}_{ss}$ by the curvature κ. In the numerical implementation, the curvature singularities can be alleviated using extrapolations or by selecting a time step that does not coincide exactly with the curvature singular points. This can always be achieved because the RMT-curve analysis is performed at a post-processing step. However, by using the Frenet angles, a proof of existence of the unit normal $\mathbf{n}$ can be provided since the Frenet bank angle always exists regardless of the magnitude of the curve curvature.

3. Frenet bank, vertical-development, and curvature angles

In this section, the Frenet angles are introduced using the general curve geometry described in the preceding section. This serves to provide geometric interpretations of these angles and to generalize the more specialized analysis presented in the literature [25, 26].

3.1 Frenet bank angle

The Frenet frame is defined by the three unit vectors $\mathbf{r}_s, \mathbf{n}$, and $\mathbf{b}$, where $\mathbf{b} = \mathbf{r}_s \times \mathbf{n}$ is the bi-normal vector [13 – 18]. The $\mathbf{r}_s - \mathbf{n}$ plane is the *osculating plane* in which the velocity and acceleration vectors lie, and for this reason, it is referred to in this study as the *motion plane*. The bi-normal vector $\mathbf{b}$ is orthogonal to the motion plane and serves as its normal. The centrifugal force in its totality is always along the normal vector $\mathbf{n}$. The $\mathbf{r}_s - \mathbf{b}$ plane is the *rectifying plane* which contains the velocity vector and the tangential component of the acceleration vector, and has $\mathbf{n}$ as its normal. The $\mathbf{n} - \mathbf{b}$ plane is the *normal plane* which contains the normal component of the acceleration vector, and has the unit tangent $\mathbf{r}_s$ as its normal.

Important in this investigation is a recognition that the normal plane can be defined by the two orthogonal unit vectors $\mathbf{n}$ and $\mathbf{b}$, or alternatively, by the two unit vectors $\mathbf{n}_1$ and $\mathbf{n}_2$. This is clear because the unit tangent vector $\mathbf{r}_s$ is orthogonal to the two $\mathbf{n} - \mathbf{b}$ and $\mathbf{n}_1 - \mathbf{n}_2$ sets of vectors. That is, these two sets of vectors lie in the same planar surface, and they differ by a single rotation about $\mathbf{r}_s$ unit vector. This rotation is the *Frenet bank angle* ϕ, which defines the *Frenet super-elevation* of the motion-trajectory curve. As shown in the preceding section, $\mathbf{n} = (1/\kappa)\mathbf{r}_{ss}$, and $\mathbf{n}_1$, and $\mathbf{n}_2$ are defined in Eq. 6, where κ is the RMT-curve curvature. Therefore, the following two equations define the Frenet bank angle

$$\cos\phi = \mathbf{n}\cdot\mathbf{n}_1 = \left(\kappa_h/\kappa\right), \quad \sin\phi = \mathbf{n}\cdot\mathbf{n}_2 = \left(-\kappa_v/\kappa\right) \tag{9}$$

In this study, κ_h is referred to as the *Frenet horizontal curvature* since it is defined along the unit vector $\mathbf{n}_1$ which lies in a plane parallel to the horizontal plane, while κ_v is referred to as the *Frenet vertical-development curvature* , referred to for brevity as the *vertical curvature*, because it is along the vector $\mathbf{n}_2$ which is vertical if the motion plane is not vertically elevated ($z' = 0$). The frame formed by the three vectors $\mathbf{r}_s, \mathbf{n}_1$, and $\mathbf{n}_2$ is referred to in this study as the *Frenet pre-super-elevated frame*, and the $\mathbf{r}_s - \mathbf{n}_1$ plane is referred to as the *pre-super-elevated osculating plane* (PSEO). It is important to observe that while the two vectors $\mathbf{n}_1$ and $\mathbf{n}_2$ lie in the normal plane, the planar surface defined by these two vectors remains perpendicular to the unit tangent $\mathbf{r}_s$ regardless of the Frenet bank angle rotation, which is an Euler rotation performed along an axis in the direction of $\mathbf{r}_s$.

3.2 Frenet vertical-development angle

The unit vector $\mathbf{n}_1$, defined in Eq. 6, lies in a plane parallel to the horizontal plane and it forms, with the unit tangent vector $\mathbf{r}_s$, the Frenet PSEO plane. Nonetheless, the PSEO plane is not, in general, a planar surface that is parallel to the horizontal plane. This is clear from the general definition of the unit tangent vector $\mathbf{r}_s$. Using the definition of the vector $\mathbf{n}_1$ which lies in a plane parallel to the horizontal plane, it is clear that the PSEO plane differs from the horizontal plane by a single rotation θ about the $-\mathbf{n}_1$ vector, where the negative sign is used to keep the notations consistent with what is used in the railroad vehicle literature [24 – 26]. The angle θ is referred to in this study as the *Frenet vertical-development angle*. Without this Frenet-Euler rotation, the unit tangent vector lies in the horizontal plane and is defined by the equation

$\mathbf{r}_{sb} = \begin{bmatrix} 1 & y' & 0 \end{bmatrix}^T \Big/ \sqrt{1+(y')^2}$, which is a unit vector orthogonal to $\mathbf{n}_1$. In this special *pre-vertical-development configuration*, the vector $\mathbf{n}_2$ occupies a position defined by the equation $\mathbf{n}_{2b} = \mathbf{r}_{sb} \times \mathbf{n}_1 = \begin{bmatrix} 0 & 0 & 1 \end{bmatrix}^T = \mathbf{k}$, which is a unit vector along the vertical Z axis. Therefore, recalling that $\mathbf{n}_2 = \left(1 \Big/ |\mathbf{r}_x| \sqrt{1+(y')^2}\right) \begin{bmatrix} -z' & -y'z' & 1+(y')^2 \end{bmatrix}^T$, the *Frenet vertical-development angle* is defined by the following two equations:

$$\left.\begin{aligned} \cos\theta &= \mathbf{k} \cdot \mathbf{n}_2 = \sqrt{1+(y')^2} \Big/ |\mathbf{r}_x| \\ \sin\theta &= (\mathbf{A}_\theta \mathbf{k})_1 = z' \Big/ |\mathbf{r}_x| \end{aligned}\right\} \tag{10}$$

where subscript one refers to the first element in the product $\mathbf{A}_\theta \mathbf{k}$ and $\mathbf{A}_\theta$ is the orthogonal transformation matrix defined using Rodrigues formula with $-\mathbf{n}_1$ as the axis of rotation as [24]

$$\mathbf{A}_\theta = \mathbf{I} - \tilde{\mathbf{n}}_1 \sin\theta + 2(\tilde{\mathbf{n}}_1)^2 \sin^2(\theta/2) \tag{11}$$

where $\mathbf{I}$ is the 3×3 identity matrix and $\tilde{\mathbf{n}}_1$ is the skew-symmetric matrix associated with the unit vector $\mathbf{n}_1$. It is clear from the definition of the Frenet vertical-development angle θ that if $z' = 0$, this angle is zero, and $\kappa_v = 0$ justifying calling κ_v *Frenet vertical curvature*. It is important to keep in mind that derivatives in the equations presented in this section are defined with respect to the curve coordinate x and not with respect to an arc-length coordinate. Using the definitions presented in this section, the derivative of the Frenet vertical-development angle θ can be written as $\theta' = \left(z''\left(1+(y')^2\right) - y'y''z'\right) \Big/ \left(|\mathbf{r}_x|^2 \sqrt{1+(y')^2}\right)$. In Appendix A of the paper, more discussion on the vectors $\mathbf{n}_1$ and $\mathbf{n}_2$ is provided.

3.3 Frenet curvature angle

Before the Frenet super-elevation or Frenet vertical-elevation, the curve unit-tangent vector is defined by the equation $\mathbf{r}_{sb} = \begin{bmatrix} 1 & y' & 0 \end{bmatrix}^T \Big/ \sqrt{1+(y')^2}$. This equation describes a planar curve on the horizontal plane. The *Frenet curvature angle* ψ is defined by the two equations

$$\cos\psi = 1\Big/\sqrt{1+(y')^2}, \quad \sin\psi = y'\Big/\sqrt{1+(y')^2} \tag{12}$$

Using these definitions, the vector $\mathbf{r}_{sb}$ can be written as $\mathbf{r}_{sb} = \begin{bmatrix} \cos\psi & \sin\psi & 0 \end{bmatrix}^T$, which shows that the angle ψ can be considered as a rotation about the vertical Z axis that brings the vector $\begin{bmatrix} 1 & 0 & 0 \end{bmatrix}^T$ to the vector $\mathbf{r}_{sb} = \begin{bmatrix} \cos\psi & \sin\psi & 0 \end{bmatrix}^T$. One can also show that $\psi' = y''\Big/\left(1+(y')^2\right)$. The curvature vector of the planar curve is defined as $\mathbf{r}_{ssb} = \left(\psi'/|\mathbf{r}_x|\right)\begin{bmatrix} -\sin\psi & \cos\psi & 0 \end{bmatrix}^T$, which shows that the curvature of this planar curve is $\psi'/|\mathbf{r}_x| = y''\Big/\left(|\mathbf{r}_x|\left(1+(y')^2\right)\right)$, which is the same as the Frenet horizontal curvature if $z' = 0$, which is the case of the planar curve considered. The equation for ψ' can then be written as $\psi' = y''\Big/\left(1+(y')^2\right)$.

4. Normal vector and curvature singularity

The design of the rail-track or highway-ramp super-elevations are based on the assumption that the vehicle strictly traces a circular curve that lies in a plane parallel to the horizontal plane. This case corresponds to non-zero rail-track or highway-ramp bank angle and to a zero Frenet bank angle. This assumption is violated in most realistic motion scenarios because of the vehicle lateral displacements. Such assumption of zero Frenet bank angle can only be made if, for example, a rail vehicle slides up or down and maintains continuous contact with the high or low rail, respectively. This situation, often encountered in practice, is not desirable for two main reasons. First, it is an

indication that the condition of the balance speed fails to keep the vehicle centered on the track. Second, because of the continuous wheel/rail contact, the high or low rail is subjected to high flange contact forces that can lead to deterioration and wear of the wheel and rail surfaces, undesirable track movements, and the possibility of wheel climbs and derailments. Computer simulations and observations of realistic motion scenarios have shown that indeed the balance speed does not always maintain the vehicle centered and does not prevent wheel/rail flange contact with significantly high impact forces.

4.1 Direction of the normal vector

The condition required for a vehicle to trace a curve that lies in a plane parallel to the horizontal plane can be met only under certain geometric restrictions. From the definition of the curvature vector $\mathbf{r}_{ss}$, it is clear that the centrifugal force remains in a plane parallel to the horizontal plane if the condition $z''+y'\left(z''y'-z'y''\right)=0$ is satisfied. That is,

$$z''/z' = y''y'\Big/\left(1+\left(y'\right)^2\right) \tag{13}$$

If this condition is satisfied, the normal vector and the centrifugal force remain in a plane parallel to the horizontal plane. Furthermore, this condition shows that the centrifugal force can remain in a plane parallel to the horizontal plane (zero Frenet super-elevation) for non-zero vertical-elevation (non-zero Frenet vertical-elevation).

The helix curve is an example in which the condition of Eq. 13 is satisfied. The helix is curved, twisted, vertically-elevated, but not Frenet super-elevated [25, 26]. The equation of the helix is $\mathbf{r}\left(s\right)=\left[a\cos\alpha \quad a\sin\alpha \quad b\alpha\right]^T$, where $\alpha = s\Big/\sqrt{a^2+b^2}$, s is the arc length parameter, a is the helix radius, $r=\sqrt{\left(a\right)^2+\left(b\right)^2}$, and b/a is the slope of the helix. The helix curvature κ and torsion

τ are constant and defined, respectively, as $\kappa = |a| \big/ \left(a^2 + b^2\right)$ and $\tau = b \big/ \left(a^2 + b^2\right)$. Using the equation $x = a\cos\alpha = a\cos\left(s/r\right)$, one has

$$\left.\begin{aligned} &\cos\alpha = x/a, \quad \sin\alpha = \sqrt{1-\left(x/a\right)^2} \\ &dx = -\left[\left(a/r\right)\sin\alpha\right] ds \end{aligned}\right\} \tag{14}$$

Using these identities, the vector $\mathbf{r}_x$ is defined for the helix as

$$\begin{aligned} \mathbf{r}_x &= \mathbf{r}_s \left(\partial s/\partial x\right) = \left[x' \quad y' \quad z'\right]^T \\ &= \left[1 \quad -1/\tan\alpha \quad -b \big/ \left(a\sin\alpha\right)\right]^T \end{aligned} \tag{15}$$

This equation defines

$$\left.\begin{aligned} &y' = -1/\tan\alpha, \quad z' = -b \big/ \left(a\sin\alpha\right), \quad \left|\mathbf{r}_x\right| = r \big/ \left(a\sin\alpha\right) \\ &y'' = -1/a\sin^3\alpha, \quad z'' = -\left(b \big/ \left(a\right)^2\right)\left(\cos\alpha/\sin^3\alpha\right) \end{aligned}\right\} \tag{16}$$

To check the condition $z''/z' = y'y'' \big/ \left(1+\left(y'\right)^2\right)$, one has $z''/z' = \left(\cos\alpha/a\sin^2\alpha\right)$, $y'y'' = \cos\alpha/a\sin^4\alpha$, $1+\left(y'\right)^2 = 1/\sin^2\alpha$, and $y'y'' \big/ \left(1+\left(y'\right)^2\right) = \left(\cos\alpha/a\sin^2\alpha\right)$, which demonstrates that indeed the condition $z''/z' = y'y'' \big/ \left(1+\left(y'\right)^2\right)$ is satisfied, implying that the curved, twisted, and vertically-elevated helix has a normal that always lies in a plane parallel to the horizontal plane. This fact can be simply demonstrated by directly differentiating the unit tangent vector $\mathbf{r}_s$ to obtain the curvature vector $\mathbf{r}_{ss} = \partial^2\mathbf{r}/\partial s^2 = -\left(a/r^2\right)\left[\cos\alpha \quad \sin\alpha \quad 0\right]^T$. Therefore, a vehicle negotiating a helix has a centrifugal inertia force that always lies in a plane parallel to the horizontal plane, and such a force cannot be balanced by the vertical gravity forces if the helix geometry is not altered. The helix example also demonstrates that the centrifugal force

can remain in a plane parallel to the horizontal plane for a vertically-elevated curve which has non-zero vertical-development angle θ, that is, $\theta \neq 0$.

4.2 Existence of the unit normal vector

The unit vector $\mathbf{n}$ normal to the curve is defined using the curvature vector $\mathbf{r}_{ss}$ as $\mathbf{n} = \mathbf{r}_{ss}/\kappa$. At the *curvature singular points*, the curve curvature κ is equal to zero, and therefore, the unit normal vector cannot be defined using the equation $\mathbf{n} = \mathbf{r}_{ss}/\kappa$. The Frenet angles can be used to prove the existence of the unit normal vector and provide a definition of this vector regardless of whether or not the value of the curve curvature is zero. It is clear from the analysis presented in this section that the Frenet curvature and vertical-development angles depend on the first derivatives and are not function of the curvature. The Frenet bank angle, on the other hand, which defines the Frenet super-elevation, depends on the curvature and is defined by the equations $\phi = \tan^{-1}\left(-\kappa_v/\kappa_h\right)$, which shows that $\phi = \tan^{-1}\left(0/0\right)$. Using the definition of κ_v and κ_h, the condition of the curvature singular points $y'' = z'' = 0$, and L'Hopital's rule, one can show that the Frenet bank angle can be defined from the curvature ratio

$$\kappa_v/\kappa_h = \left(z'''\left(1+\left(y'\right)^2\right) - y'z'y'''\right)\Big/\left(y'''\left|\mathbf{r}_x\right|\right) \tag{17}$$

Because all the Frenet angles exist and using their definitions, the unit vector $\mathbf{n}$ normal to the curve can always be written in terms of the Frenet angles as [24 – 26]

$$\mathbf{n} = \begin{bmatrix} -\sin\psi\cos\phi + \cos\psi\sin\theta\sin\phi \\ \cos\psi\cos\phi + \sin\psi\sin\theta\sin\phi \\ -\cos\theta\sin\phi \end{bmatrix} \tag{18}$$

This expression for the normal vector is defined at all curve points including the curvature singular points. Therefore, the direction of the centrifugal inertia force is well defined even at the curve

points at which the curvature is zero. This is demonstrated by the analytical example considered in a later section in which a curve with curvature singularities is considered.

5. Frenet inertia forces

Experimentally or simulation *recorded motion trajectory* (RMT) curves can be used to define an inverse problem in which the inertia force can be expressed in terms of the curve parameters. To distinguish this form of the inertia force based on a Cartesian representation, the curve-based definition of the inertia forces is referred to as the *Frenet inertia forces*. Differentiating $\mathbf{r} = \mathbf{r}(s)$ once and twice with respect to time leads, respectively, to the velocity and acceleration vectors $\dot{\mathbf{r}} = \dot{s}\mathbf{r}_s$ and $\ddot{\mathbf{r}} = \begin{bmatrix} \ddot{x} & \ddot{y} & \ddot{z} \end{bmatrix}^T = \left((\dot{s})^2 / R \right) \mathbf{n} + \mathbf{r}_s \ddot{s}$, where $\mathbf{n} = \mathbf{r}_{ss} / \kappa = R\mathbf{r}_{ss}$ is the unit normal vector. Therefore, the inertia force vector of a vehicle with mass m tracing a curve can be written as

$$\mathbf{F}_i = m\ddot{\mathbf{r}} = m\begin{bmatrix} \ddot{x} & \ddot{y} & \ddot{z} \end{bmatrix}^T = m\left(\left((\dot{s})^2 / R \right) \mathbf{n} + \ddot{s}\mathbf{r}_s \right) \tag{19}$$

where $R = R(s)$ is the curve radius of curvature.

5.1 Velocity, acceleration, and curvature vector

If the vehicle has arbitrary forward velocity $\dot{x}$, the tangential velocity $\dot{s}$ along the tangent $\mathbf{r}_s$ is

$$\dot{s} = \partial s / \partial t = |\dot{\mathbf{r}}| = \dot{x}\sqrt{1 + (y')^2 + (z')^2} = \dot{x}|\mathbf{r}_x| \tag{20}$$

This equation shows that $ds = |\dot{\mathbf{r}}| dt = \left(|\dot{\mathbf{r}}| / \dot{x} \right) dx$. The component of the acceleration $\ddot{s}$ along the tangent to the curve can be obtained by differentiating $\dot{s}$ as $\ddot{s} = \dot{s}\left(d\dot{s} / ds \right) = \ddot{x}|\mathbf{r}_x| + \dot{x}\left(d|\mathbf{r}_x| / dt \right)$. This equation leads to

$$\begin{aligned} \ddot{s} &= \left(\ddot{x}|\mathbf{r}_x|^2 + (\dot{x})^2 (y'y'' + z'z'') \right) \Big/ |\mathbf{r}_x| = \left(\ddot{x}|\mathbf{r}_x|^4 + (y'y'' + z'z'')(\dot{s})^2 \right) \Big/ |\mathbf{r}_x|^3 \\ &= \left(\ddot{x}|\mathbf{r}_x|^2 + \alpha_c (\dot{s})^2 \right) \Big/ |\mathbf{r}_x| = \left(\ddot{x} + (\dot{x})^2 \alpha_c \right) |\mathbf{r}_x| \end{aligned} \tag{21}$$

which shows that if $\dot{x}$ is constant, $\ddot{s}$ is not zero and $\dot{s}$ is not constant since the tangent vector varies as function of x, or equivalently as function of t. It is clear from the definition of $\ddot{s}$ that at a *curvature singular point* defined by the condition $y'' = z'' = 0$, $\ddot{s} = \ddot{x}\left|\mathbf{r}_x\right|$ because $\alpha_c = \left(y'y'' + z'z''\right)\Big/\left|\mathbf{r}_x\right|^2 = 0$, as previously mentioned,

Using the definitions of $\dot{s}$ and $\ddot{s}$, one has the following identities:

$$\left.\begin{aligned} 1 + \left(y'\right)^2 + \left(z'\right)^2 &= \left|\mathbf{r}_x\right|^2 = \left(\dot{s}/\dot{x}\right)^2 \\ y'y'' + z'z'' &= \left(\dot{s}\Big/\left(\dot{x}\right)^2\right)\left(\left(\ddot{s}\dot{x} - \dot{s}\ddot{x}\right)\Big/\left(\dot{x}\right)^2\right) \end{aligned}\right\} \tag{22}$$

The second identity shows that, at the curvature singular points, the following relationship between the tangential and forward velocities and acceleration is satisfied

$$\ddot{s}/\dot{s} = \ddot{x}/\dot{x} \tag{23}$$

Furthermore, in the case of constant forward velocity $\dot{x} = V$, the same identities can be used to show that the curvature vector can be written in terms of $\dot{s}$ and $\ddot{s}$ in the following different forms:

$$\begin{aligned} \mathbf{r}_{ss} &= \frac{1}{\left|\mathbf{r}_x\right|^4}\left(-\left(y'y'' + z'z''\right)\begin{bmatrix}1\\ y'\\ z'\end{bmatrix} + \left(1 + \left(y'\right)^2 + \left(z'\right)^2\right)\begin{bmatrix}0\\ y''\\ z''\end{bmatrix}\right) \\ &= \frac{1}{\left(V\right)^2\left|\mathbf{r}_x\right|^2}\left(\left(V\right)^2\begin{bmatrix}0\\ y''\\ z''\end{bmatrix} - \left(\ddot{s}/\left|\mathbf{r}_x\right|\right)\begin{bmatrix}1\\ y'\\ z'\end{bmatrix}\right) \\ &= \frac{1}{\left(V\right)^2\left|\mathbf{r}_x\right|^2}\begin{bmatrix}-\left(\ddot{s}/\left|\mathbf{r}_x\right|\right)\\ \left(V\right)^2 y'' - \left(\ddot{s}/\left|\mathbf{r}_x\right|\right)y'\\ \left(V\right)^2 z'' - \left(\ddot{s}/\left|\mathbf{r}_x\right|\right)z'\end{bmatrix} = \frac{V}{\left(\dot{s}\right)^2}\begin{bmatrix}-\left(\ddot{s}/\dot{s}\right)\\ Vy'' - \left(\ddot{s}/\dot{s}\right)y'\\ Vz'' - \left(\ddot{s}/\dot{s}\right)z'\end{bmatrix} \end{aligned} \tag{24}$$

In this special case, the curvature κ is defined as the magnitude of the above curvature vector as

$$\kappa = \left(V\Big/\left(\dot{s}\right)^2\right)\sqrt{\left(V\right)^2\left(\left(y''\right)^2 + \left(z''\right)^2\right) - \left(\ddot{s}/V\right)^2} \tag{25}$$

The fact that $\mathbf{r}_s$ is a unit vector implies that $\mathbf{r}_s \cdot \mathbf{r}_{ss} = 0$, which when used with the above definition of the curvature vector $\mathbf{r}_{ss}$ shows that, when $\dot{x}$ is constant, $\ddot{s} = \left(\left(y'y'' + z'z'' \right) \left(\dot{s} \right)^2 / \left| \mathbf{r}_x \right|^3 \right)$; an expression that can be obtained from the general definition of $\ddot{s}$. Using the definition of the curvature in the special case of constant forward velocity and recognizing that the curvature is positive, the limit on the maximum acceleration of vehicle negotiating a curve can be obtained as

$$\ddot{s} \le \sqrt{\left(V \right)^4 \left(\left(y'' \right)^2 + \left(z'' \right)^2 \right)} = \left(V \right)^2 \sqrt{\left(y'' \right)^2 + \left(z'' \right)^2} \tag{26}$$

This equation defines the limit on magnitude of $\ddot{s}$, which depends on the forward velocity V.

5.2 Cartesian- and Frenet-representation of the inertia forces

The Cartesian and Frenet forms of the inertia force are equivalent. The Cartesian form is often used in a forward-dynamics problem, while the Frenet form can be used in an inverse-dynamics problem if the RMT curves are available from experimental measurements or computer simulations. The inertia force in its Cartesian form, for an arbitrary $\dot{x}$, can be written as

$$\mathbf{F}_i = m \begin{bmatrix} \ddot{x} & \ddot{y} & \ddot{z} \end{bmatrix}^T = m \left(\ddot{x} \mathbf{r}_x + \left(\dot{x} \right)^2 \mathbf{r}_{xx} \right) \tag{27}$$

The component of this force along the tangent vector is defined using the definition of $\ddot{s}$ as

$$\begin{aligned} \left| \mathbf{F}_{it} \right| &= \mathbf{F}_i \cdot \mathbf{r}_s = m \left(\ddot{x} \mathbf{r}_x \cdot \mathbf{r}_s + \left(\dot{x} \right)^2 \mathbf{r}_{xx} \cdot \mathbf{r}_s \right) \\ &= m \left(\left(\ddot{x} \left| \mathbf{r}_x \right| \right) + \left(\left(\dot{x} \right)^2 / \left| \mathbf{r}_x \right| \right) \left(y'y'' + z'z'' \right) \right) = m \ddot{s} \end{aligned} \tag{28}$$

This result is consistent with the equation $\mathbf{F}_i = m \ddot{\mathbf{r}} = m \left(\left(\left(\dot{s} \right)^2 / R \right) \mathbf{n} + \mathbf{r}_s \ddot{s} \right)$. Equation 2 shows that $\left| \mathbf{r}_x \right|^2 \mathbf{r}_{ss} = -\alpha_c \mathbf{r}_x + \mathbf{r}_{xx}$. Using this identity and the fact that $\mathbf{r}_{ss} = \kappa \mathbf{n}$ and $\dot{s} = \dot{x} \left| \mathbf{r}_x \right|$, the component of the inertia force along the normal to the curve is defined as

$$\begin{aligned}\mathbf{F}_{in} &= \mathbf{F}_i - \left(\mathbf{F}_i \cdot \mathbf{r}_s\right)\mathbf{r}_s = m\left(\ddot{x}\mathbf{r}_x + \left(\dot{x}\right)^2 \mathbf{r}_{xx}\right) - m\ddot{s}\mathbf{r}_s \\ &= m\left(\dot{x}\right)^2\left(\mathbf{r}_{xx} - \alpha_c \mathbf{r}_x\right) = m\left(\dot{x}\right)^2 \left|\mathbf{r}_x\right|^2 \kappa\mathbf{n} = m\left(\left(\dot{s}\right)^2 / R\right)\mathbf{n}\end{aligned} \tag{29}$$

This equation defines the centrifugal force in its totality when the vehicle negotiates a curve. The preceding two equations demonstrate the equivalence of the Cartesian and Frenet forms of the inertia force vector and also show that the norm of the acceleration vector can be written as $\left|\ddot{\mathbf{r}}\right| = \sqrt{\left(\ddot{\mathbf{r}} \cdot \ddot{\mathbf{r}}\right)} = \sqrt{\left(\ddot{s}\right)^2 + \left(\kappa\left(\dot{s}\right)^2\right)^2}$.

5.3 Centrifugal force and horizontal plane

In practice, track super-elevations are designed with the assumption that the centrifugal force remains in a plane parallel to the horizontal plane [26]. Using this assumption, the balance speed is determined by equating the lateral components of the gravity and centrifugal forces. According to this assumption, the vehicle strictly follows a circle that lies in a plane parallel to the horizontal plane, a condition that cannot be met in realistic motion scenarios because of the lateral displacements. The actual motion trajectories can represent sharp curves with large curvature values. The orientation of the *osculating* (motion) *plane* that contains the velocity and acceleration vectors, defines the direction of the centrifugal force. If the osculating plane is not Frenet super-elevated, the centrifugal force remains in a plane parallel to the horizontal plane. To show that the condition $z''/z' = y'y''\Big/\left(1+\left(y'\right)^2\right)$ implies zero Frenet bank angle ϕ, one can rewrite

$$\left.\begin{aligned}\cos\phi &= \left(\kappa_h/\kappa\right) = y''\Big/\left(\kappa\left|\mathbf{r}_x\right|^2\sqrt{1+\left(y'\right)^2}\right), \\ \sin\phi &= \left(-\kappa_v/\kappa\right) = -\left(z''\left(1+\left(y'\right)^2\right) - z'y'y''\right)\Big/\left(\kappa\left|\mathbf{r}_x\right|^3\sqrt{1+\left(y'\right)^2}\right)\end{aligned}\right\} \tag{30}$$

These two equations show that if $z''/z' = y'y''\Big/\left(1+\left(y'\right)^2\right)$, $\sin\phi = 0$ and $\cos\phi = 1$, providing a proof that under this condition the osculating plane is not Frenet super-elevated.

6. Coordinate selection and inertia forces

While the vehicle motion is described in terms of a large number of coordinates, an RMT curve is one dimensional, and consequently, the motion of the center of mass of a vehicle component, as represented by one RMT curve, is described in terms of one coordinate if the curve geometry is known from experimentally or simulation recorded data. Use of RMT curves is equivalent to using an *inverse-dynamics problem* in which the motion is assumed to be partially or fully prescribed and the goal is to determine the forces that produce this motion. Therefore, the nonlinear-dynamics analysis approach used in this paper is different from the classical inverse problem in which the prescribed motion is used to determine constraint forces that produce the motion. In this paper, on the other hand, the assumption is made that the forces exerted on the vehicle are the *actual forces*, and such forces are not determined with the goal of producing specified motion. The RMT curves, therefore, are the solution of a forward-dynamics problem in which the applied forces are not pre-computed and should not be viewed as control forces. Nonetheless, such RMT curves have all motion characteristics and can be used to extract information that cannot be obtained or easily understood using other approaches.

If the motion of the vehicle center of mass is described using the three-dimensional vector $\mathbf{r} = \begin{bmatrix} x & y & z \end{bmatrix}^T$, the coordinates x, y, and z in the forward dynamics problem can be considered as independent if they are not related by constraint equations. However, RMT curve can be written in terms of one parameter, which can be time t, arc length s, or any other parameter including the curve coordinates x, y, and z. For example, if the curve longitudinal coordinate x is used as the curve parameter, one can write $\mathbf{r} = \mathbf{r}(x) = \begin{bmatrix} x & y(x) & z(x) \end{bmatrix}^T$. This equation implies that the

motion in the inverse problem is subjected to two kinematic constraints $y = y(x)$ and $z = z(x)$. If the equation of motion of the vehicle center of mass is written in the forward-dynamics problem in response to a force vector $\mathbf{F}$ using the Cartesian coordinates as $m\ddot{\mathbf{r}} = \mathbf{F}$, this equation can be described in the inverse-dynamics problem using the RMT curve in terms of one parameter only. To this end, one can write, as previously described, $\dot{\mathbf{r}} = \dot{x}\begin{bmatrix}1 & y' & z'\end{bmatrix}^T$, if the coordinate x is used as the curve parameter. This equation leads to

$$\begin{aligned}\ddot{\mathbf{r}} &= \ddot{x}\begin{bmatrix}1 & y' & z'\end{bmatrix}^T + (\dot{x})^2\begin{bmatrix}0 & y'' & z''\end{bmatrix}^T \\ &= \mathbf{B}_{di}\ddot{x} + (\dot{x})^2\,\bar{\mathbf{v}}\end{aligned} \tag{31}$$

In this equation, $\mathbf{B}_{di} = \mathbf{r}_x = \begin{bmatrix}1 & y' & z'\end{bmatrix}^T$ is a velocity transformation that reduces to the tangent vector, which is not in general a unit vector; and $\bar{\mathbf{v}} = \begin{bmatrix}0 & y'' & z''\end{bmatrix}^T$ is a vector that lies in the lateral $y-z$ plane. Substituting the preceding equation into the three equations of motion $m\ddot{\mathbf{r}} = \mathbf{F}$ and pre-multiplying by the transpose of the transformation matrix $\mathbf{B}_{di}$, one obtains a single equation of motion which can be written as $m\left(1+(y')^2+(z')^2\right)\ddot{x} = \mathbf{r}_x^T\mathbf{F} - m(\dot{x})^2(y'y''+z'z'')$. By using another coordinate y or z as the curve parameter and following a similar procedure, one obtains a similar equation associated with the other parameter. Therefore, one has the following different forms of the equation of motion if the vehicle traces the curve:

$$\left.\begin{aligned} m\left(1+(y')^2+(z')^2\right)\ddot{x} &= \mathbf{r}_x^T\mathbf{F} - m(\dot{x})^2(y'y''+z'z''), \quad a' = \partial a/\partial x \\ m\left((x')^2+1+(z')^2\right)\ddot{y} &= \mathbf{r}_y^T\mathbf{F} - m(\dot{y})^2(x'x''+z'z''), \quad a' = \partial a/\partial y \\ m\left((x')^2+(y')^2+1\right)\ddot{z} &= \mathbf{r}_z^T\mathbf{F} - m(\dot{z})^2(x'x''+y'y''), \quad a' = \partial a/\partial z \end{aligned}\right\} \tag{32}$$

Which shows that when x, y, or z is selected as the curve parameter, there is a quadratic-velocity inertia force defined by the term $-m\left(\dot{a}\right)^2\left(\mathbf{r}_a \cdot \mathbf{r}_{aa}\right)$, $a = x, y, z$. If the gravity is the only force applied to the vehicle, the preceding equation reduces to

$$m\left|\mathbf{r}_a\right|^2 \ddot{a} = \begin{bmatrix} 0 & 0 & -mg \end{bmatrix}^T \mathbf{r}_a - m\left(\dot{a}\right)^2\left(\mathbf{r}_a \cdot \mathbf{r}_{aa}\right),\ a = x, y, z \tag{33}$$

where g is the gravity constant.

It was shown previously that $\ddot{\mathbf{r}} = \ddot{s}\mathbf{r}_s + \left(\left(\dot{s}\right)^2 / R\right)\mathbf{n}$, where in this case the velocity transformation matrix becomes $\mathbf{B}_{di} = \mathbf{r}_s$. Using this velocity transformation and following the procedure used with the coordinate x, one can show that the equation of motion when s is selected as the curve parameter is given by $m\ddot{s} = \mathbf{r}_s^T\mathbf{F}$. Because $\mathbf{r}_s$ and $\mathbf{r}_{ss}$ are orthogonal vectors, the equation $m\ddot{s} = \mathbf{r}_s^T\mathbf{F}$ does not show any quadratic-velocity inertia forces, shedding light on the effect of the selection of the coordinates in the inverse-dynamics problem on the interpretation of the inertia forces. The centrifugal force $m\left(\left(\dot{s}\right)^2 / R\right)$ is a quadratic-velocity inertia force, but such a force does not appear in the equation of motion $m\ddot{s} = \mathbf{r}_s^T\mathbf{F}$ because the motion is not allowed along the normal or the bi-normal to the curve.

7. Recorded motion trajectories (RMT)

Using computational dynamics algorithms or experimental measurements, the motion trajectories of the vehicle components can be recorded and used in an inverse problem to extract the geometry and force equations presented in the preceding sections. The steps of the procedure for accomplishing this goal can be summarized as follows:

1. The position, velocity, and acceleration vectors defined, respectively, by the vectors $\mathbf{r}, \dot{\mathbf{r}}$, and $\ddot{\mathbf{r}}$ are recorded as function of time. That is, $\mathbf{r} = \mathbf{r}(t) = \begin{bmatrix} x & y & z \end{bmatrix}^T$, $\dot{\mathbf{r}} = \dot{\mathbf{r}}(t) = \begin{bmatrix} \dot{x} & \dot{y} & \dot{z} \end{bmatrix}^T$, and $\ddot{\mathbf{r}} = \ddot{\mathbf{r}}(t) = \begin{bmatrix} \ddot{x} & \ddot{y} & \ddot{z} \end{bmatrix}^T$. Experimental measurements or computer simulations based on the solution of a forward dynamics problem can be used to determine the position, velocity, and acceleration curves.
2. The curve arc length s can be determined by integrating the equation $ds = |\dot{\mathbf{r}}|\, dt$ and the absolute velocity of the vehicle component along the tangent vector can be determined from the equation $\dot{s} = |\dot{\mathbf{r}}|$. If the forward velocity of the vehicle $\dot{x}$ is different from zero, $\dot{s} = |\dot{\mathbf{r}}| > 0$. This condition is satisfied as the vehicle continues to move forward, which is the assumption made in this paper.
3. The unit tangent vector to the curve $\mathbf{r}_s$ is determined from the equation

$$\mathbf{r}_s = \begin{bmatrix} \partial x/\partial s & \partial y/\partial s & \partial z/\partial s \end{bmatrix}^T = \dot{\mathbf{r}}/|\dot{\mathbf{r}}| \tag{34}$$

   It is also clear that

$$\mathbf{r}_x = \begin{bmatrix} 1 & y' & z' \end{bmatrix}^T = \dot{\mathbf{r}}/\dot{x} \tag{35}$$

   This equation can be used to define y' and z'. Because $\dot{x}$ is known from the recorded velocity, the vector $\mathbf{r}_x$ can be determined. A similar procedure can be used to determine $\mathbf{r}_y$ and $\mathbf{r}_z$ if the velocities $\dot{y}$ and $\dot{z}$ are different from zero.
4. Because $\ddot{\mathbf{r}} = \ddot{s}\mathbf{r}_s + \left((\dot{s})^2 / R \right) \mathbf{n}$ and because $\mathbf{r}_s$ and $\mathbf{n}$ are orthogonal vectors, the acceleration $\ddot{s}$ can be defined using the equation $\ddot{s} = \ddot{\mathbf{r}} \cdot \mathbf{r}_s$ and the radius of curvature R is determined from the equation $R = (\dot{s})^2 / (\ddot{\mathbf{r}} \cdot \mathbf{n})$, where $\mathbf{n}$ is computed in the following step. The equation

$R = (\dot{s})^2 / (\ddot{\mathbf{r}} \cdot \mathbf{n})$ should be used with care at the curvature singular points. The curvature of the RMT curve is defined as $\kappa = 1/R$.

5. The equation $\ddot{\mathbf{r}} = \ddot{s}\mathbf{r}_s + \left((\dot{s})^2 / R\right)\mathbf{n}$ shows that the unit normal vector $\mathbf{n}$ is parallel to the vector $\mathbf{n} = \left(R/(\dot{s})^2\right)(\ddot{\mathbf{r}} - \ddot{s}\mathbf{r}_s)$. That is,

$$\mathbf{n} = (\ddot{\mathbf{r}} - \ddot{s}\mathbf{r}_s) / |\ddot{\mathbf{r}} - \ddot{s}\mathbf{r}_s| \tag{36}$$

6. Using the recorded velocities and accelerations, and the equations previously developed in this study, one can show that

$$\begin{bmatrix} 0 & y'' & z'' \end{bmatrix}^T = \left(1/(\dot{x})^2\right)(\ddot{\mathbf{r}} - \ddot{x}\mathbf{r}_x) \tag{37}$$

That is, the second derivative with respect to the parameter x can be determined. Using these second derivatives, the vertical curvature κ_v and the horizontal curvature κ_h can be computed. As check, the curvature κ can be written in the alternate form $\kappa = \sqrt{(\kappa_v)^2 + (\kappa_h)^2}$.

7. The RMT Frenet-Euler angles can then be determined from the equations

$$\left.\begin{aligned} &\cos\psi = 1/\sqrt{1+(y')^2}, \quad \sin\psi = y'/\sqrt{1+(y')^2}, \\ &\cos\theta = \sqrt{1+(y')^2}/|\mathbf{r}_x|, \quad \sin\theta = z'/|\mathbf{r}_x|, \\ &\cos\phi = (\kappa_h/\kappa) = y''/\left(\kappa|\mathbf{r}_x|^2\sqrt{1+(y')^2}\right), \\ &\sin\phi = (-\kappa_v/\kappa) = -\left(z''\left(1+(y')^2\right) - z'y'y''\right)/\left(\kappa|\mathbf{r}_x|^3\sqrt{1+(y')^2}\right) \end{aligned}\right\} \tag{38}$$

8. The PSEO plane is defined by the two orthogonal vectors $\mathbf{n}_1$ and $\mathbf{n}_2$ of Eq. 6, which can be determined using the derivatives defined by the RMT data.

9. The inertia forces on the vehicle component can be determined in the global Cartesian coordinate system as $m\ddot{\mathbf{r}}$. The projection of this inertia force along the RMT normal $\mathbf{n}$ can be

determined as $m\ddot{\mathbf{r}}\cdot\mathbf{n}=m\left(\dot{s}\right)^2/R$, while the projection of the inertia force along the tangent vector $\mathbf{r}_s$ is determined using $m\ddot{\mathbf{r}}\cdot\mathbf{r}_s=m\ddot{s}$.

10. Because the gravity force can be written in the global coordinate system as $\mathbf{F}_g=-mg\begin{bmatrix}0 & 0 & 1\end{bmatrix}^T$, an estimate of other forces $\mathbf{F}_{eo}$, including constraint forces, acting on the vehicle component can be written as $\mathbf{F}_{eo}=m\ddot{\mathbf{r}}-\mathbf{F}_g$. In the case of tangent track sections, the elements of the vector $\mathbf{F}_{eo}$ define forces in the longitudinal, lateral, and vertical directions. The vector $\mathbf{F}_{eo}$ can be projected along the axes of the Frenet frame to define the components $\mathbf{F}_{eo}\cdot\mathbf{r}_s$, $\mathbf{F}_{eo}\cdot\mathbf{n}$, and $\mathbf{F}_{eo}\cdot\mathbf{b}$. Because, there is no inertia force along the bi-normal vector $\mathbf{b}$, one must have $\left(\mathbf{F}_{eo}+\mathbf{F}_g\right)\cdot\mathbf{b}=0$. If the effect of the gravity is not considered, $\mathbf{F}_{eo}\cdot\mathbf{b}=0$.

Using the steps and equations of this procedure is demonstrated in the numerical-example section using an analytical space curve which has curvature singular points.

8. Frenet oscillations and numerical results

In this section, a numerical example of an analytical space curve is considered to demonstrate use of MT data to obtain the geometry and force equations developed in this study. The example is used to demonstrate that simple MT curves give rise to centrifugal forces, and such forces are not attributed to road or track geometry, but to the MT geometry. The example considered also demonstrates how the Frenet-Euler angles can be determined using RMT-curve data.

8.1 Curve geometry

The three-dimensional MT curve, which is assumed to represent a vehicle travelling with a constant forward velocity V, is defined as

$$\begin{aligned}\mathbf{r} = \begin{bmatrix} x & y & z \end{bmatrix}^T &= \begin{bmatrix} Vt & Y_h \sin(\omega_h t) & Z_{ho} + \gamma Y_h \sin(\omega_h t) \end{bmatrix}^T \\ &= \begin{bmatrix} x & Y_h \sin(\omega_h x/V) & Z_{ho} + \gamma Y_h \sin(\omega_h x/V) \end{bmatrix}^T \end{aligned} \tag{39}$$

where Y_h and Z_h are given amplitudes, ω_h is the frequency, $x = Vt$, and $V = \partial x / \partial t$. In this example, $Y_h = 0.02$ m, $V = 15$ m/s, $\gamma = 1/20$, $\omega_h = \alpha_h V = 5.9$ rad/s $= 0.939$ Hz, $\alpha_h = 0.3935$ m, and $Z_{ho} = 2$ m. It is clear from the definition of the curve that the coordinate z is related to the curve coordinate y by the linear relationship $z = Z_{ho} + \gamma y$, and $z = Z_{ho}$ when $y = 0$. For simplicity, the results are reported in this section using time t as a parameter.

The curve velocity vector is

$$\begin{aligned}\dot{\mathbf{r}} = \mathbf{r}_t = \begin{bmatrix} \dot{x} & \dot{y} & \dot{z} \end{bmatrix}^T &= \begin{bmatrix} V & \omega_h Y_h \cos \omega_h t & \omega_h \gamma Y_h \cos \omega_h t \end{bmatrix}^T \\ &= V \begin{bmatrix} 1 & \alpha_h Y_h \cos \omega_h t & \alpha_h \gamma Y_h \cos \omega_h t \end{bmatrix}^T \end{aligned} \tag{40}$$

Using this velocity vector, one has

$$\dot{s} = |\dot{\mathbf{r}}| = V \sqrt{1 + (\alpha_h Y_h)^2 \left(1 + (\gamma)^2\right) \cos^2 \omega_h t} \tag{41}$$

This equation shows that the velocity $\dot{s}$ along the tangent to the MT curve is always larger than the velocity $\dot{x} = V$ along the curve parameter x. The velocity $\dot{s}$ is maximum at the peaks of the curve when $\omega_h t = \omega_h x / V = n\pi, n = 1, 2, \ldots$. At these points, $\dot{s} = 19.000465$ m/s. It is also clear that $\dot{s} = \dot{x} = V$ when $\omega_h t = \omega_h x / V = (n+1)\pi/2, n = 0, 2, 4, \ldots$. Figure 2 shows the velocity $\dot{s}$ as a function of time. The oscillatory nature of $\dot{s}$ is clear from the results presented in this figure.

Using the MT velocity vector $\dot{\mathbf{r}}$ and the computed velocity $\dot{s}$, one can write

$$\left.\begin{aligned} \mathbf{r}_x &= \begin{bmatrix} 1 & y' & z' \end{bmatrix}^T = \dot{\mathbf{r}}/V \\ &= \begin{bmatrix} 1 & \alpha_h Y_h \cos \omega_h t & \alpha_h \gamma Y_h \cos \omega_h t \end{bmatrix}^T \\ |\mathbf{r}_x| &= \sqrt{1 + (\alpha_h Y_h)^2 \left(1 + (\gamma)^2\right) \cos^2 \omega_h t} \end{aligned}\right\} \tag{42}$$

The unit tangent vector $\mathbf{r}_s$ can be determined using the RMT vector as

$$\mathbf{r}_s = \dot{\mathbf{r}}/\dot{s} = \left(V/\dot{s}\right)\begin{bmatrix}1 & \alpha_h Y_h \cos\omega_h t & \alpha_h \gamma Y_h \cos\omega_h t\end{bmatrix}^T \tag{43}$$

Figure 3 shows the X-elements of the unit tangent vector $\mathbf{r}_s$, which is the dominant component. While other elements of the tangent vector were found to be very small, the three elements of the unit tangent $\mathbf{r}_s$ are oscillatory. The absolute acceleration vector for the curve considered in this section is

$$\ddot{\mathbf{r}} = d\dot{\mathbf{r}}/dt = \begin{bmatrix}\ddot{x} & \ddot{y} & \ddot{z}\end{bmatrix}^T = -\left(\omega_h\right)^2 Y_h \begin{bmatrix}0 & \sin\omega_h t & \gamma\sin\omega_h t\end{bmatrix}^T \tag{44}$$

Using the acceleration vector $\ddot{\mathbf{r}}$, the acceleration $\ddot{s}$ along the tangent to the curve can be evaluated using the equation

$$\ddot{s} = \ddot{\mathbf{r}}\cdot\mathbf{r}_s = -\left(\left(\omega_h\right)^3\left(Y_h\right)^2\left(1+\left(\gamma\right)^2\right)\Big/2\dot{s}\right)\sin\left(2\omega_h t\right) \tag{45}$$

Figure 4 shows $\ddot{s}$ as a function of time. It is clear that while the forward velocity V is constant, $\ddot{s}$ is not zero and it is oscillatory with a small amplitude. The acceleration $\ddot{s}$ is the acceleration component along the tangent to the curve. The curvature κ of a curve is defined to be the magnitude of the curvature vector, and in the case of a spatial curve is assumed to be positive. In the case of planar curves, a sign can be given to the curvature to indicate how the normal vector is oriented. Figure 5 shows the curvature κ, the horizontal curvature κ_h, and the vertical curvature κ_v. The results presented in this figure show the curvature singular points which are points of discontinuities of the curvature κ. The radius of curvature R at an arbitrary point can be determined from the equation $R = 1/\kappa$. The results presented in Fig. 5 demonstrate that, even simple oscillations can result in curves with very small radius of curvatures. Federal railroad

regulations, for example, put limit on the radius of curvature of the tracks. Such limits, however, cannot be imposed on MT curves which are not a priori known.

8.2 Force analysis

The direction of the centrifugal force is defined by the direction of the unit vector $\mathbf{n}$ normal to the curve. The results obtained using the example considered in this section shows that the *Y*-component of the normal vector is dominant, while the other two components are oscillatory, but with small amplitudes. The results presented in Fig. 6, which shows the *Y*-component of the normal vector, explain the dominance of the lateral component. Figure 7 shows the Frenet bank angle ϕ which defines the Frenet super-elevation of the motion (osculating) plane which contains the velocity and acceleration vectors as well as the centrifugal-force vector. At the point $t = 0$, which is a curvature singular point, one can use the L'Hopital's rule as described in the paper to show that at this point, $\phi \approx -2.862°$. A Frenet bank angle in the range of $3°$ is not considered small when the projection of forces of heavy vehicles are considered since a small error can lead to significant unbalance force. Figure 8 shows the Frenet curvature angle ψ and vertical-development angle θ for the space curve considered in this section.

Small oscillations with very large inertia are not uncommon in vehicle system applications. For example, in the case of railroad vehicle systems, 100-ton car of a freight train experiences hunting oscillations with amplitude that can be less or exceed the amplitude considered in this example. The frequency $\omega_h = \alpha_h V = 5.9$ rad/s $= 0.939$ Hz considered in this section corresponds to a forward velocity of 15 m/s which is a relatively low speed for both passenger and freight trains. While the analytical space curve considered in this section does not duplicate the actual behavior of a railroad vehicle whose complex motion requires use of the techniques of constrained multibody system (MBS) dynamics, the qualitative analysis using such an analytical curve can

shed light on the significance of the Frenet oscillations introduced in this study. Figure 9 shows the magnitude of the centrifugal force $m(\dot{s})^2/R$ for a 100-ton car tracing the curve used in this section. This is the total magnitude of the centrifugal force which has the same direction of the unit vector $\mathbf{n}$ normal to the curve. The figure also shows the projection of the magnitude of the centrifugal force on the horizontal plane as defined by the equation $\left(m(\dot{s})^2/R\right)\cos\phi$ and the vertical component as defined by $\left(m(\dot{s})^2/R\right)\sin\phi$. It is clear from the results presented in this figure that the vertical component is small and the horizontal component is dominant.

As discussed in this paper, oscillatory centrifugal forces arise in cases the highway roads or rail tracks are not super-elevated. Even in these cases, the gravity force can have a component that opposes the centrifugal force which is in the direction of the unit vector $\mathbf{n}$ normal to the curve. In many application, particularly in the case of conical railroad wheelsets, the conicity produces self-steering that leads to geometric self-centering as the result of force self-balancing. Figure 10 shows the component of the gravity force $\mathbf{F}_g \cdot \mathbf{n}$ along the normal to the curve. It is clear from the results presented in this figure that gravity force has a component that lies in the motion (osculating) plane of the curve, and such a gravity component is in a direction opposite to the direction of the centrifugal force.

9. Discussion and relationship to previous work

As discussed in this paper, the Frenet bank angle ϕ defines deviation of the plane of the centrifugal force from the horizontal plane regardless of the geometry of the railroad track or the highway road. If the Frenet bank angle ϕ is equal to zero, the centrifugal force and the vector normal to the curve lie in a plane parallel to the horizontal plane. This angle also defines the magnitude of the

component of the gravity force that opposes the centrifugal force in its totality. For example, a curve can be vertically elevated (developed), but is not Frenet super-elevated. The helix is a good example of such a curve. If a particle traces a helix curve, the gravity force cannot balance the centrifugal force. Therefore, the Frenet bank angle ϕ in addition to having a clear geometric meaning, it also has a clear physical interpretation. More investigations are needed to study the impact of these new definitions on the interpretation of the forces that produce the motion.

The analysis presented in this paper shows clearly that Eq. 9 should not be used to determine the Frenet bank angle ϕ in case of zero curvature. The angle ϕ can be determined at the singular curvature point using Eq. 17. The results presented in Fig. 7 for a curve with a large number of zero-curvature points demonstrate that the Frenet bank angle is continuous and the unit vector normal to the curve is well defined. Equation 17, therefore, provides a proof that the normal to the curve is well defined at the points of zero curvatures. Consequently, there is no discontinuity in the definition of the Frenet frame. This proof could be developed using the concept of the horizontal and vertical curvatures used in the railroad vehicle literature and the definitions of the Frenet angles.

As previously stated, this investigation builds on previous studies [25, 26], which were not concerned with the analysis of recorded motion trajectories and the curvature singularities. This paper presents new derivations and identities, establishes a data-driven science approach and algorithm for utilization of recorded motion trajectories to interpret motion and forces, provides a proof that demonstrates that the Frenet frame does not suffer from any discontinuities at zero-curvature points, and develops a simple analytical curve to obtain new results that demonstrate concepts that have not previously discussed in the literature. The three-dimensional curve analysis presented in this paper is also different from the analysis presented in a newly published study

which is focused on $x-y$ curve which has zero Frenet vertical-development angle θ and zero Frenet bank angle ϕ [27].

10. Conclusions

Computer simulations and physical measurements can be used to record positions, velocities, and accelerations of moving bodies. The RMT curves, which are the results of actual forces or nonlinear virtual prototyping of credible computer models, have information that can shed light on the system nonlinear dynamics. In this paper, a mechanics-based description of the curve geometry is developed and used to introduce the *Frenet oscillations*, which define the time-varying characteritics of the *motion plane*. The motion (osculating) plane contains the absolute velocity and acceleration vectors and its orientation can be systematically described in terms of the three *Frenet-Euler angles*; the *curvature*, *vertical-development*, and *bank angles*. The *Frenet super-elevation* of the motion plane measures the deviation of the direction of the centrifugal inertia force from the horizontal plane. The paper uses Frenet angles to introduce a method to determine the unit vector normal to a curve at the curvature singular points. The definition of this normal vector is necessary in order to define the correct direction of the centrifugal force. To better understand the motion-plane oscillations, the concept of the *pre-super-elevated osculating (PSEO) plane* is introduced. A new *inverse-dynamics problem* that utilizes experimentally or simulation *recorded motion trajectories* (RMT) is formulated and used to define the *Frenet inertia forces*. The equivalence of the Frenet inertia forces and the Cartesian form of the inertia forces is shown. The Frenet inertia forces can include a quadratic-velocity inertia force vector if a curve parameter different from the arc length is used. The recorded velocity and acceleration vectors can be used to obtain new expressions for the *curvature vector*. The paper defines the limit on the magnitude

of the tangential acceleration for a given forward velocity and the condition that must be met for the centrifugal force to lie in a plane parallel to the horizontal plane. The results obtained using a simple analytical curve example demonstrate the *Frenet oscillations* and the importance of distinguishing between the highway-ramp and railroad *track bank angle* and super-elevation, which are time-invariant, and the *Frenet bank angle* and super-elevation, which are oscillatory. The latter defines the correct direction of the centrifugal forces. While an analytical MT curve is considered to demonstrate the Frenet oscillations and curvature singular points, more detailed MBS models will be the subject of future investigations focused on the hunting oscillations of railroad vehicle systems and the interpretation of the Frenet-Euler angles and Frenet oscillations in complex motion scenarios.

The sequence of rotations $Z,-Y,-X$ used in this investigation is the sequence adopted by the transportation industry for the construction of the geometry and layout of highway roads and railroad tracks. This sequence when applied to the recorded motion-trajectory curves allows introducing concepts of the horizontal curvature, vertical-development, and super-elevation used in the description of the track geometry by the railroad industry. Use of this sequence, therefore, allows comparing and distinguishing the geometry of the motion trajectories from the geometry of the road and the track because similar concepts are used. Nonetheless, many of the equations and identities presented in this paper can have counterparts that may assume different forms if another sequence of rotations, including the *Bishop frame*, is used [28]. For example, Tait-Bryan angles widely used in vehicle and flight dynamics as well as the Z,X,Z sequence used by Euler to study the gyroscopic motion can be used to provide similar development and identities that will assume different forms depending on the sequence used. While, nonlinear relationships between different angles based on different sequences of rotations can always be developed, the Tait-Bryan sequence

and the Z, X, Z sequence used by Euler do not provide the simple geometric interpretation provided by the sequence of rotations adopted in this paper. Furthermore, the Frenet-angle sequence used in this study demonstrates clearly that the curve can be completely defined using two independent angles, which serve as alternatives to the curvature and torsion in defining the curve geometry. The coordinates of a curve $\mathbf{r}$ can be determined by integrating the equation $d\mathbf{r} = \mathbf{r}_s ds$, demonstrating that the curve coordinates can be expressed in terms of the two independent angles. Use of another angle sequence can lead to a unit tangent expressed in terms of three angles instead of two and such angles may not have the same geometric interpretation as the one used by the rail industry.

Appendix A

Pre-super-elevated-osculating (PSEO) plane

One can show that the two orthogonal vectors $\mathbf{n}_1$ and $\mathbf{n}_2$ can be obtained by, respectively, applying the following two transformations, which are not necessarily orthogonal, to the unit tangent $\mathbf{r}_s$:

$$\mathbf{T}_1 = \frac{|\mathbf{r}_x|}{\sqrt{1+(y')^2}}\begin{bmatrix} 0 & -1 & 0 \\ 1 & 0 & 0 \\ 0 & 0 & 0 \end{bmatrix}, \qquad \mathbf{T}_2 = \frac{1}{\sqrt{1+(y')^2}}\begin{bmatrix} 0 & 0 & -1 \\ 0 & -z' & 0 \\ 1 & y' & 0 \end{bmatrix} \tag{A.1}$$

That is, the two orthogonal unit vectors $\mathbf{n}_1$ and $\mathbf{n}_2$ can be determined using the first derivatives that appear in the tangent vector. In this case, the scalars κ_h and κ_v can be determined, respectively, using the dot products $\kappa_h = \mathbf{r}_{ss} \cdot \mathbf{n}_1$ and $\kappa_v = \mathbf{r}_{ss} \cdot \mathbf{n}_2$. These two curvature components can be used to determine the curve curvature and radius of curvature. It is also important to note that the three vectors $\mathbf{r}_s, \mathbf{n}_1$, and $\mathbf{n}_2$ are three orthogonal vectors, as discussed in the paper.

The two vectors $\mathbf{n}_1$ and $\mathbf{n}_2$ have an interesting geometric interpretation. These two vectors lie in a plane whose normal is defined by the unit tangent vector $\mathbf{r}_s$ which represents the axis of rotation of the Frenet bank angle ϕ. This means that any other vector that lies in the plane formed by the two vectors $\mathbf{n}_1$ and $\mathbf{n}_2$ can still be written as a linear combination of the two orthogonal vectors $\mathbf{n}_1$ and $\mathbf{n}_2$ before or after the Frenet bank angle rotation ϕ. As discussed in the paper, the two orthogonal vectors $\mathbf{n}_1$ and $\mathbf{n}_2$ are the normal and binormal vectors of the Frenet frame before performing the Frenet bank-angle rotation. Furthermore, the projection of the inertia forces along the two orthogonal unit vectors $\mathbf{n}_1$ and $\mathbf{n}_2$ can be used to conveniently define the centrifugal force, as explained in the paper.

Acknowledgements

This research was supported by the National Science Foundation (Project # 1632302).

Compliance with Ethical Standards:

The author declares that they have no conflict of interest

Data Availability Statement

The datasets generated during and/or analysed during the current study are available from the corresponding author on reasonable request.

REFERENCES

1. Li, B., Ma, H., Yu, X. *et al.*, 2019, "Nonlinear Vibration and Dynamic Stability Analysis of Rotor-Blade System with Nonlinear Supports", *Archive of Applied Mechanics*, Vol. 89**,** pp. 1375 – 1402, https://doi.org/10.1007/s00419-019-01509-0.
2. Wright, J.A., Bartuccelli, M., Gentile, G., 2017, "Comparisons between the Pendulum with Varying length and the pendulum with oscillating support", *Journal of Mathematical Analysis and Applications*, Vol. 449(2), pp. 1684 – 1707.
3. Younesian, D., Hosseinkhani, A., Askari, H., Esmailzadeh, E, 2019, "Elastic and Viscoelastic Foundations: A Review on Linear and Nonlinear Vibration Modeling and Applications", *Nonlinear Dynamics*, Vol. 97, pp. 853 – 895.
4. Yang, W., Towfighian, S., 2017, "A Hybrid Nonlinear Vibration Energy Harvester", *Mechanical Systems and Signal Processing*, Vol. 90, pp. 317 – 333.
5. Haris, A., Alevras, P., Mohammadpour, M. *et al.*, 2020, "Design and Validation of a Nonlinear Vibration Absorber to Attenuate Torsional Oscillations of Propulsion Systems", *Nonlinear Dynamics*, Vol. 100**,** pp. 33 – 49, https://doi.org/10.1007/s11071-020-05502-z.
6. Timoshenko, S., Young, D. H., and Weaver, W., 1974, *Vibration Problems in Engineering*, Wiley, New York.
7. Shabana, A.A., 2019, *Vibration of Discrete and Continuous Systems*, Third Edition, Springer, New York.
8. Hu, H.Y., and Wang, Z.H., 2002, *Dynamics of Controlled Mechanical Systems with Delayed Feedback*, Springer, Berlin, Germany.
9. Aslanov, V.S., 2019, "Stability of a Pendulum with a Moving Mass: The Averaging Method", *Journal of Sound and Vibration*, Vol. 445, pp. 261 – 269.

10. Carpineto, N., Lacarbonara, W., Vestroni, F., ,2014, "Hysteretic Tuned Mass Dampers for Structural Vibration Mitigation", *Journal of Sound and Vibration*, Vol. 333, pp. 1302 – 1318.
11. Tkhai, V., 2020, "Stabilizing the Oscillations of a Controlled Mechanical System with *n* Degrees of Freedom". *Autom Remote Control*, Vol. 81**,** pp. 1637–1646.
12. Lacarbonara, W., and Cetraro, M., 2011, "Flutter Control of a Lifting Surface via Visco-Hysteretic Vibration Absorbers", *International Journal of Aeronautical & Space Science*, Vol. 12(4), pp. 331 – 345, DOI:10.5139/IJASS.2011.12.4.331.
13. Farin, G., 1999, *Curves and Surfaces for CAGD*, A Practical Guide, Fifth Edition, Morgan Kaufmann, Publishers, San Francisco.
14. Gallier, J., 2011, *Geometric Methods and Applications: For Computer Science and Engineering*, Springer, New York.
15. Goetz, A., 1970, *Introduction to Differential Geometry*, Addison Wesley.
16. Kreyszig, E., 1991, *Differential Geometry*, Dover Publications.
17. Piegl, L., and Tiller, W., 1997, *The NURBS Book*, Second Edition, Springer, Berlin.
18. Rogers, D.F., 2001, *An Introduction to NURBS with Historical Perspective*, Academic Press, San Diego, CA.
19. Ginsberg, J., 2008, *Engineering Dynamics*, Cambridge University Press, New York.
20. Goldstein, H., 1950, *Classical Mechanics*, Addison-Wesley.
21. Greenwood, D. T., 1988, *Principles of Dynamics*, 2nd ed., Prentice Hall, Englewood Cliffs, NJ.
22. Huston, R. L., 1990, *Multibody Dynamics*, Butterworth-Heinemann, Stoneham, MA.
23. Roberson, R. E., and Schwertassek, R., 1988, *Dynamics of Multibody Systems*, Springer-Verlag, Berlin.

24. Shabana, A.A., 2021, *Mathematical Foundation of Railroad Vehicle Systems: Geometry and Mechanics*, John Wiley & Sons.

25. Ling, H., and Shabana, A.A., 2021, "Euler Angles and Numerical Representation of the Railroad Track Geometry", *Acta Mechanica*, doi.org/10.1007/s00707-020-02903-4.

26. Shabana, A.A., and Ling, H., 2021, "Characterization and Quantification of Railroad Spiral-Joint Discontinuities", *Mechanics-Based Design of Structures and Machines*, doi.org/10.1080/15397734.2020.1855193.

27. Shabana, A.A., 2021, "Geometric Self-Centering and Force Self-Balancing of Railroad Vehicle Hunting Oscillations", *Acta Mechanica*, doi.org/10.1007/s00707-021-02983-w.

28. Khalid Jawed, M., Novelia, A., and O'Reilly, O.M., 2018, *A Primer on the Kinematics of Discrete Elastic Rods*, Springer, Cham, Switzerland.

Figure Captions

Figure 1 Frenet oscillations [26]

Figure 2 Velocity $\dot{s}$

Figure 3 *X*-component of the unit tangent to the curve

Figure 4 Acceleration $\ddot{s}$

Figure 5 Curve curvatures (Black-triangle: Curvature κ; Red-square: Horizontal curvature κ_h; Blue-circle: Vertical curvature κ_v)

Figure 6 *Y*-coordinate of the unit normal vector

Figure 7 Frenet bank angle ϕ

Figure 8 Frenet vertical-development and curvature angles (Black-triangle: θ; Red-square: ψ)

Figure 9 Centrifugal force (Black-triangle: $m(\dot{s})^2/R$; Red-square: $\left(m(\dot{s})^2/R\right)\cos\phi$; Blue-circle: $\left(m(\dot{s})^2/R\right)\sin\phi$)

Figure 10 Component of the gravity force in the osculating plane

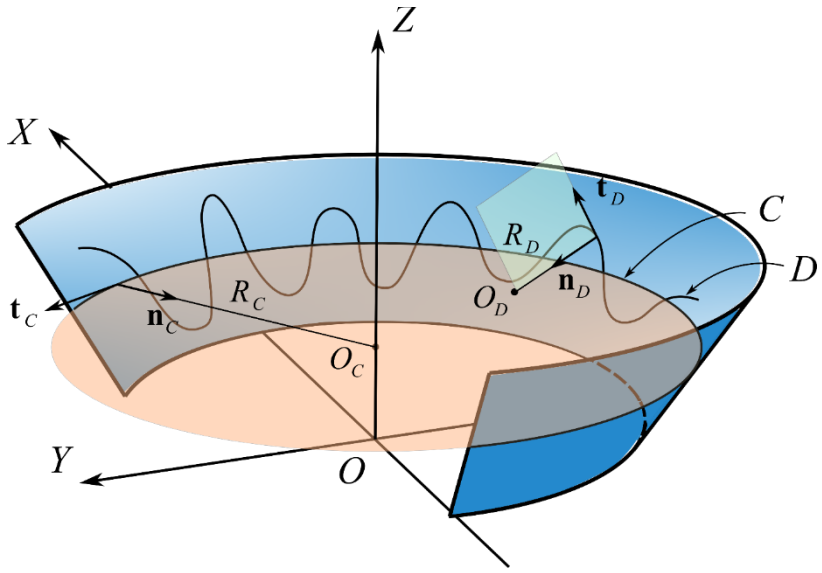

Figure 1 Frenet oscillations [26]

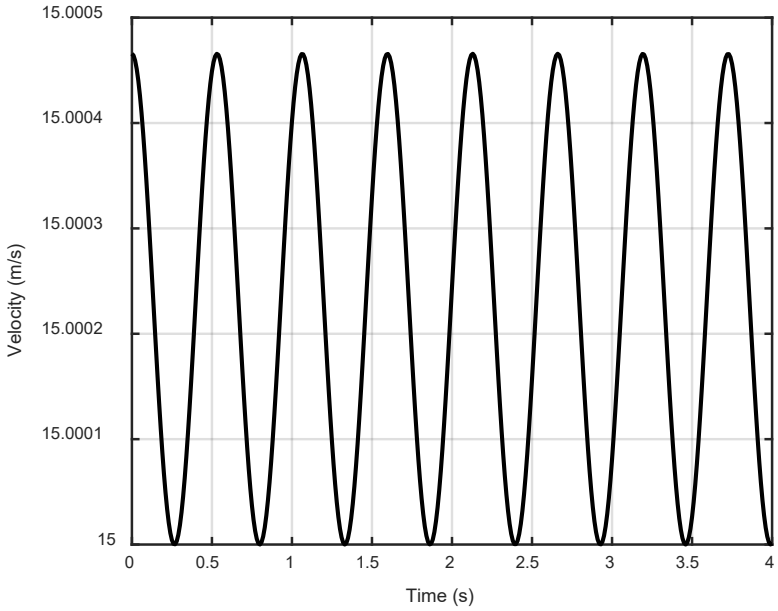

Figure 2 Velocity $\dot{s}$

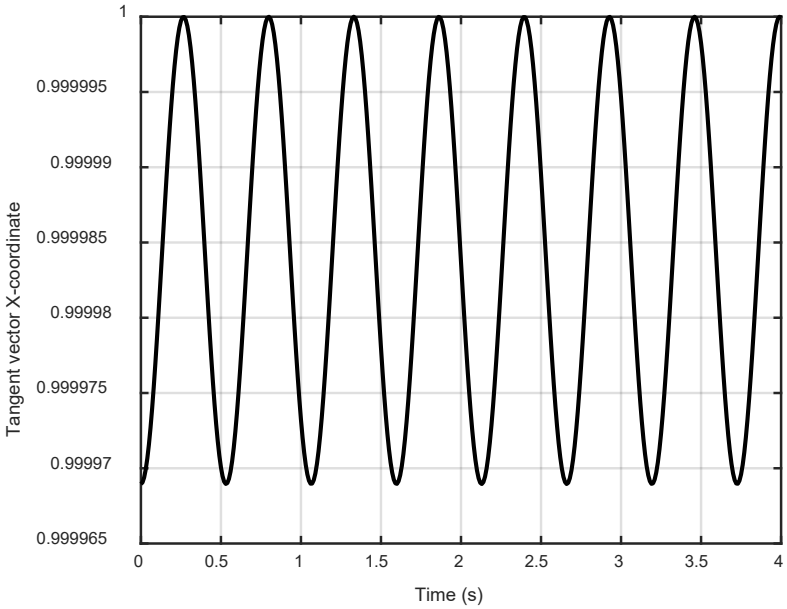

Figure 3 *X*-component of the unit tangent to the curve

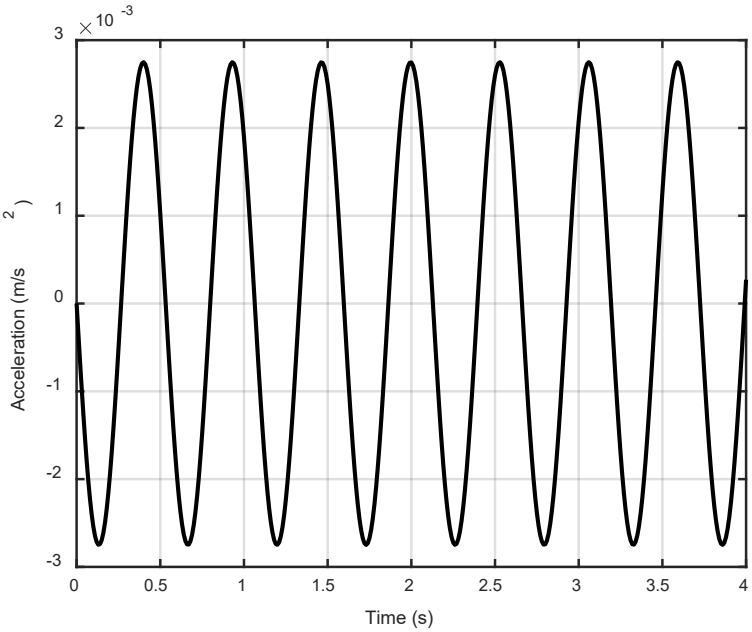

Figure 4 Acceleration $\ddot{s}$

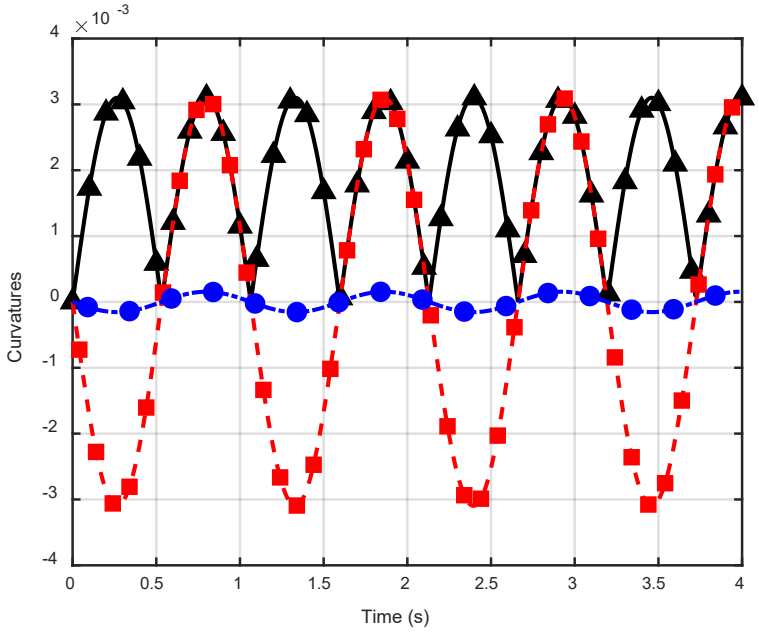

Figure 5 Curve curvatures (Black-triangle: Curvature κ ; Red-square: Horizontal curvature κ_h ; Blue-circle: Vertical curvature κ_v)

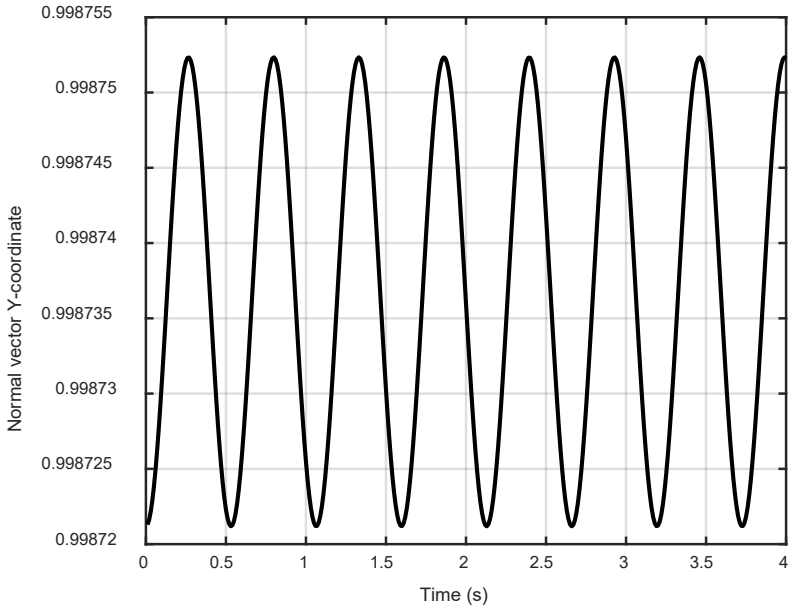

Figure 6 *Y*-coordinate of the unit normal vector

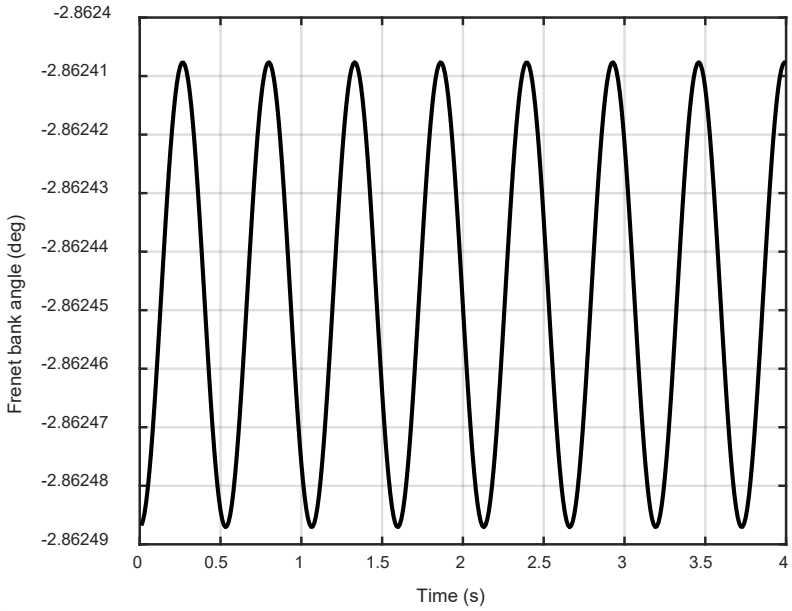

Figure 7 Frenet bank angle ϕ

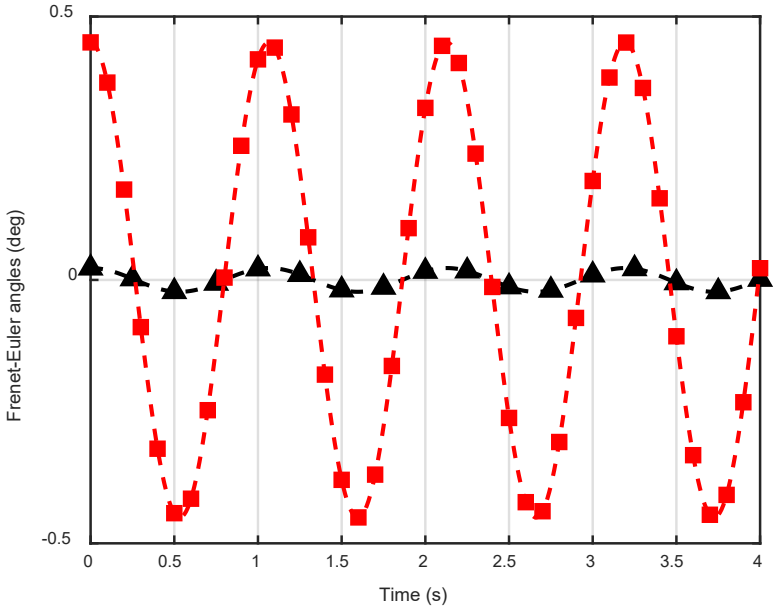

Figure 8 Frenet vertical-development and curvature angles (Black-triangle: θ; Red-square: ψ)

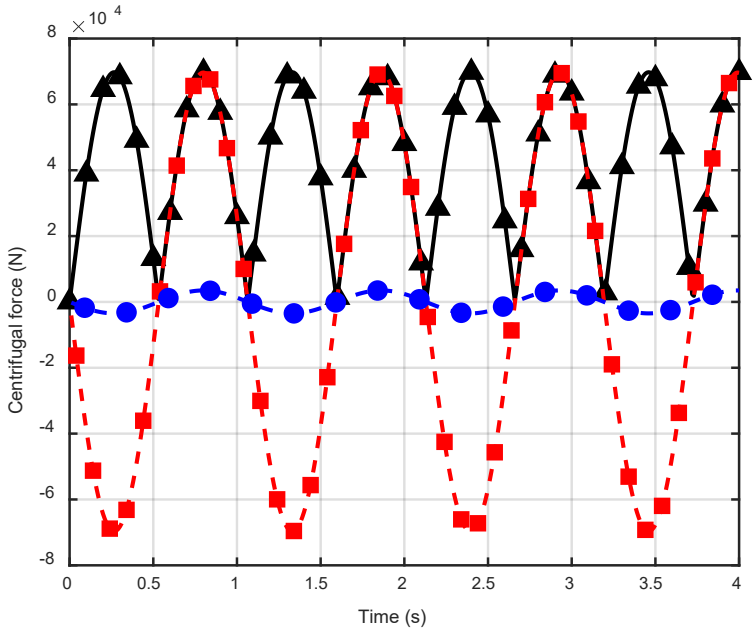

Figure 9 Centrifugal force (Black-triangle $m(\dot{s})^2/R$; Red-square: $\left(m(\dot{s})^2/R\right)\cos\phi$; Blue-circle: $\left(m(\dot{s})^2/R\right)\sin\phi$)

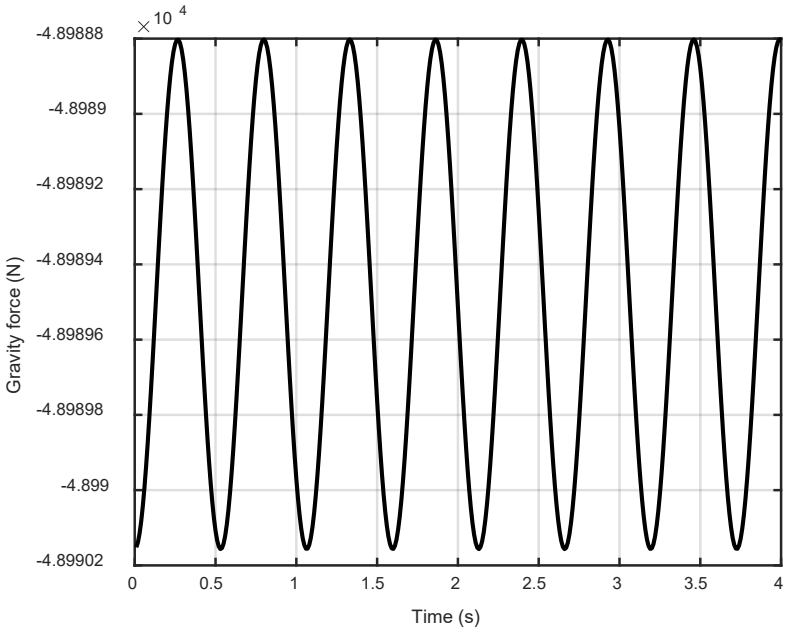

Figure 10 Component of the gravity force in the osculating plane